Title: Nitrogen-doped Seamless Activated Carbon Electrode with Excellent Durability for Electric Double Layer Capacitor

Author Names: Tomomi Tagaya,[a] Yoshikiyo Hatakeyama,[a] Soshi Shiraishi,[a,*,z] Hidehiko Tsukada,[b] María José Mostazo-López,[c] Emilia Morallón,[d] Diego Cazorla-Amorós[c]

Affiliation(s): [a]Division of Molecular Science, Graduate School of Science and Technology, Gunma University, Kiryu 376-8515, Japan, [b]AION Co. Ltd., Koga 306-0213, Japan, [c]Departamento de Química Inorgánica and Instituto Universitario de Materiales, Universidad de Alicante, Spain

[d]Departamento de Química Física and Instituto Universitario de Materiales, Universidad de Alicante, Spain

[z]Corresponding Author E-mail Address [soshishiraishi3@gunma-u.ac.jp]

[*]Membership status

Abstract Text [200 Words or Less] [Required]

Electric double layer capacitor (EDLC) using seamless activated carbon electrode shows excellent durability against high voltage charging, compared with conventional activated carbon composite electrode. In this paper, the authors focused on nitrogen-doping as surface modification to further improve the electrochemical durability of the seamless electrode. The EDLC using the nitrogen-doped seamless activated carbon electrode achieved the volumetric capacitance of 18 F cm^{-3} (under the galvanostatic method, 80 mA, 0–2.5 V, 40 °C) and the capacitance retention of 83 % after the floating durability test (3.5 V, 70 °C, 100 h) using a typical propylene carbonate electrolyte. The volumetric capacitance is comparable to that (14 F cm^{-3}) of the conventional activated carbon such as YP50F, and the retention is much higher than that (76%) of pristine seamless activated carbon. The authors concluded that the extremely excellent durability of nitrogen-doped seamless activated carbon electrode is due to (i) the stable electric network arising from the binder-less monolithic structure and (ii) nitrogen-doped chemical state that suppress pore blocking and internal resistance change caused by electrochemical decomposition deposits. (175 words)

Introduction

For suitable energy forms, electric double layer capacitors (EDLCs) have received considerate attention as electric energy storage.[1,2] The charge/discharge mechanism is based on ion adsorption/desorption at the electric double layer between electrolyte and nanoporous carbon electrode such as activated carbon. This non-faradic process brings fast charge/discharge as well as high power and long cycle life compared with batteries that based on faradaic process. However, the energy density of EDLC is lower than that of rechargeable batteries. Here, the energy stored in EDLC is proportional to the capacitance and the square of charge voltage. Therefore, the capacitance and maximum charge voltage should be increased to improve the energy density. As for increasing capacitance, many studies have been dedicated to optimize the pore structure of nanoporous carbon to increase the capacitance. However, this approach has limitation on the volumetric capacitance of activated carbons because micropore development by activation decreases the electrode bulk density.[2–4] Another way to increase capacitance is adding pseudocapacitance based on transition metal oxides, polymers, and surface functionalities.[1,2,5,6] However, the pseudocapacitance materials generally suffer from poor electrochemical stability because redox reactions are used.[1,2] Then, the cell voltage should be expanded for higher energy density. However, the high voltage charging causes to deteriorate EDLC. Therefore, the improvement of the durability against high voltage charging is an indispensable strategy from viewpoint of both energy density and reliability.[3,4,7–9]

The durability of the cells against high voltage charging is mainly determined by the stability of electrolyte.[10] From the viewpoint of the potential window, organic electrolytes has more advantages than aqueous ones suffering from water electrolysis.[1] For example, the electrolytes using ammonium salts and organic solvents such as acetonitrile and propylene carbonate are widely used for commercial EDLCs because of its good conductivity, wide operating temperature and relatively high operating voltage of 2.5–3.0 V.[11,12] Furthermore, the highly electrochemical-stable electrolyte using sulfones, 3-cyanopropionic acid methyl

ester (CPAME) as solvent, or ionic liquid based on N, N-diethyl-N-methyl-N-(2-methoxyethyl)ammonium (DEME), has been actively developed.[11,13–15]

On the other hand, the electrode material is also important for high-voltage charging because the electrode affects the limitation of cell voltage due to the interaction with electrolyte and the durability of the electrode itself.[2,16–18] As a result of the interaction with electrolyte at high voltage (>3 V), activated carbon electrode deteriorates due to the pore blocking caused by the electrochemical decomposition deposits. In addition, the breakdown of the electric network inside the electrodes is a fatal problem under more aggressive conditions. Conventionally, activated carbon composite electrode for EDLC has been prepared by kneading activated carbon particles with conductive additive such as carbon black as well as binder. In this type of electrode, electric point contact between activated carbon particles is not only an origin of internal resistance but also easily broken by electrochemical decomposition under high voltage charge. For example, Komaba et al. reported that the defluorination of the poly-tetrafluoroethylene (PTFE) binder causes the degradation of EDLC at high voltage operation.[7] Meanwhile, activated carbon monolith intrinsically has no electric contacts inside. That is why it shows high electric conductivity when used as electrode.[19,20] Moreover, the authors revealed the binder-less monolithic structure gives durable electric-network against high voltage.[3,21,22] Seamless activated carbon electrode that the authors developed, which is a monolith carbon electrode, exhibits a relatively high capacitance even after high voltage charging at 3.5 V, which is an aggressive condition for conventional composite electrodes. However, the seamless activated carbon electrode still has room of further improvement on the surface property.

The stability of carbon material relies on their surface chemical state. Many studies have proved that the materials which contain small amount of defects are electrochemically stable.[1,16,18,23] However, general activated carbon has numerous defects such as edge site and oxygen-containing groups. Although the heat-treatment is known as an effective method to modify these defects, the high temperature treatment shrinks the porous structure that declines the capacitance.[4,9,24–26] Therefore, the authors have been investigating alternative surface

modification such as nitrogen (N)-doping, which can improve the high-voltage durability of EDLC using organic electrolyte.[4,25]

N-doped activated carbon is prepared by ether carbonizing nitrogen-containing precursors or reacting activated carbon with nitrogen-containing reagents.[27–29] From the viewpoint of productivity, the authors approached the latter post-treatment. The surface modification with nitrogen monoxide (NO) is a post-treatment for the N-doping to improve the electrochemically durability of activated carbon, but this method uses toxic NO gas.[4,30,31] Then, the authors found the N-doping by the post-treatment using the pyrolysis of melamine to improve the durability of the activated carbon electrode for EDLC .[32] However, this method leads to the decrease in surface area and pore volume of the activated carbon. Hence, in this paper, the authors focused on organic chemical method, which does not significantly damage the porous texture of pristine material. This N-doping is conducted with relatively easy operation under mild temperature conditions.[27]

Against these backgrounds, the authors try to improve the durability of the seamless activated carbon electrode with N-doping via organic chemical reaction. In addition, this study supports the understanding of the reason for improving durability against high voltage charging with N-doping. The previous studies for N-doping on activated carbon deal with composite electrode including carbon black and binder.[3,4,25,27], but the mechanism of the durability improvement was difficult to discuss since the deterioration factors of the EDLC cell using the composite electrode are complicated. In the case of the composite electrode, not only activated carbon and electrolyte but also conductive additives and binder have to be taken into consideration for discussing the reason for improvement of the durability against high voltage charging due to the N-doping. In this study, the seamless activated carbon electrode simplifies the discussion of the effect of the N-doping on the electrical performance because of binder-less and conductive additive-free monolithic system.

Experimental

Seamless activated carbon electrode.—Macroporous phenolic resin disk (densified MICROLITE, produced by Aion Co. Ltd., Japan) with diameter of ca. 22 mm was used as a precursor of seamless activated carbon electrode. The macropore size distribution is shown in **Fig. S1**. The precursor was carbonized at 800 °C in N_2 atmosphere for 1 h (carbonization yield: 41 %) and then activated with CO_2 at 900 °C for 4.5 h (activation yield: 55 %). The obtained seamless activated carbon electrode, henceforth "SEAMLESS", was used as starting material for N-doping.

N-doping.—N-doping on the seamless activated carbon electrode was conducted via organic chemical reaction as follows using the procedure described in the reference.[27] The pristine SEAMLESS was immersed in 1 M NH_4NO_3/ N, N-dimethylformamide (DMF) /Prydine solution (DMF: Pyridine＝1: 1) at 70 °C for 3 days under reflux. The obtained N-doped seamless activated carbon electrode, henceforth "AN-SEAMLESS", was washed with water and methanol.

Material characterization.—Scanning electron microscopic (SEM) images were taken with JSM6510AS instrument (JEOL Ltd., Japan) at acceleration voltage of 20 kV to observe the surface morphology of the electrodes. Nitrogen adsorption/desorption measurement was carried out with BELSORP28SA (MicrotracBEL Corp., Japan) at 77 K to characterize the porous texture. The samples were outgassed at 200 °C for 2 h 20 min under vacuum before the measurement. The BET specific surface area (S_{BET}) was calculated from the N_2 adsorption isotherms by using the BET equation in the 0–0.05 range of relative pressures. The micropore volume (V_{micro}) and the mean micropore-width (w_{micro}) were determined by Dubinin-Radushkevich (DR) method. The tested electrodes were evaluated after removing electrolyte as follows in the literature[8]; the electrodes were washed with propylene carbonate (PC), replaced with dimethyl carbonate and then dried at 200 °C under vacuum overnight. The elemental composition for all samples was determined by combustion analysis with MICRO CORDER JM10 (J-Science Lab Co., Ltd., Japan). X-ray photoelectron spectroscopy (XPS) for the N-doped sample was conducted using AXIS-NOVA photoelectron spectrometer (Shimizu Corp., Japan) with AlKα (15 kV, 400 W) to analyze the surface chemical state. The N1s spectra were deconvoluted by using gaussian functions with 30% of Lorentzian component. For the deconvolution, the full width at half maximum

of each peak was kept between 1.5 and 2.0 eV and a Shirley line was used for estimating the background signal.

Capacitance and durability characterization.—The seamless activated carbon electrode had disk-shape with diameter of ca. 15.5 mm and thickness of ca. 0.27 mm in average. As reference samples, composite activated carbon electrodes were prepared from typical steam-activated carbon (YP50F, Kuraray Co., Ltd., Japan) or ground SEAMLESS (gSEAMLESS), acetylene black (DENKA BLACK, Denka Co., Ltd., Japan) and PTFE-based binder (6J, Dow-Mitsui Polychemicals Co., Ltd., Japan), in weight ratio of 85: 10: 5. All electrodes were attached on etched Al foil (20C054, Japan Capacitor Industrial Co., Ltd) as current collector with conductive paste (GA715, Hitachi Chemical Co., Ltd., Japan) and then dried at 200 °C under vacuum for 2 h before cell assembly. The electrodes and typical cellulose-separators (Nippon Kodoshi Co., Japan) were immersed in 1.0 M triethylmethylammonium tetrafluoroborate ($TEMABF_4$)/PC solution (Toyo Gosei Co., Ltd., Japan) as electrolyte. Then, the capacitor test cell was assembled using Al-body two-electrode cell with the above components in argon glove box. The charge-discharge test was conducted by galvanostatic method (80–2000 mA, 0–2.5 V, 40 °C) with charge-discharge unit (HJ1001SM8A, Hokuto Denko Corp., Japan) to determine the capacitance before and after durability test. The capacitance and resistance were calculated from the charge-discharge curve in the same manner as reference.[25] The gravimetric capacitance or volumetric capacitance was determined from normalization of the observed capacitance with the total mass of activated carbon or the total electrode volume for the positive and negative electrodes. The durability test was conducted under floating condition (3.5 V, 70 °C, 100 h) with the same charge-discharge unit to accelerate the degradation. Electrochemical impedance spectroscopy (1.0×10^{-2}–2.0×10^{3} Hz, 0 V, 40 °C) was carried out before and after the durability test by potentio/galvanostat (HZ5000, Hokuto Denko Corp., Japan) and frequency Response analyzer (NF Electronic Instruments 5020).

Results and Discussion

Material characterization.—**Fig. 1** shows the SEM images of precursor disk (macroporous phenolic resin), SEAMLESS, and AN-SEAMLESS. The precursor disk has

consecutive macropores and seamless framework of phenolic resin as shown in **Fig. 1a**. This structure has been maintained even after the carbonization and activation although the disk shrunk in size (**Fig. 1b**). The N-doping did not change the macro structure at all as shown in **Fig. 1c**. The data of the microporosity, calculated by the N_2 adsorption/desorption isotherms (**Fig. 2**), was summarized in **Table I**. These isotherms are classified as typical Type I, indicating that the microporosity was developed for SEAMLESS and AN-SEAMLESS. Both of them are almost close to the conventional activated carbon powder (YP50F) for EDLC in specific surface area, micropore volume, and micropore width. Thus, in this paper, the effect of the seamless structure and the N-doping on the capacitance performance can be discussed without considering the influence of the microporosity. Moreover, the comparison in morphology and porosity between SEAMLESS and AN-SEAMLESS revealed that the N-doping does not affect the macro/microporous texture so much, while other post-treatments for N-doping to porous carbons lead to decrease in surface area and pore volume.[28]

The chemical composition and surface chemistry were characterized by combustion elemental analysis and XPS. As shown in **Table I**, both results indicate that the amount of oxygen decreased and that of nitrogen increased after the N-doping. This indicates the formation of the nitrogen-containing groups by consumption of oxygen-containing groups. The atomic ratio of nitrogen by XPS ($N/C_{XPS,}$ 2.7 %) is higher than that for the elemental analysis (N/C_{comb}, 1.0 %), so the doped nitrogen is concentrated on the electrode surface. The N1s spectrum of AN-SEAMLESS shown in **Fig. 3** is in good agreement with the previous case using KOH-activated carbons[27]. The chemical state of doped-nitrogen was determined by the spectrum deconvolution. The N1s spectrum of AN-SEAMLESS contains mainly two peaks: N1 peak at 398.6 eV assigned to pyridinic N[2,27,33] and N2 peak at 399.7 eV to amidic N[27,33]. In addition to these components, N3 peak at 400.3 eV assigned to pyrrolic N[2,27], N4 peak at 401.5 eV to quaternary N (401.3–401.8 eV) [2,27] and N5 peak at 403.5 eV to pyridinic-N-oxide[33,33] were also observed. In brief, the seamless activated carbon electrode can be N-doped with mainly pyridinic and amidic groups.

From the above results of the porosity and chemical analyses, it was elucidated that the nitrogen can be doped gently in carbon surface via organic chemical reaction to clarify the effect of the N-doping for the seamless carbon electrode.

Capacitance and Durability against high voltage charging.—**Fig. 4** shows the charge–discharge curve (80 mA g^{-1}, 0–2.5 V, 40 °C) before and after the durability test (3.5 V, 100 h, 70 °C). For all electrodes, the charge-discharge curves before the durability test were typically triangle as capacitive behavior. After the durability test, the curves of the cell using the composite electrodes (YP50F and gSEAMLESS) were distorted, while the curve shape in the cases of SEAMLESS and AN-SEAMLESS was almost maintained regardless of slight increase in the curve slope and ohmic drop at the charge and discharge process switch point. The capacitance and internal resistance calculated from the charge–discharge curves were summarized in **Table II**. Clearly, the cell using SEAMLESS exhibits very high capacitance retention (76%) and small increase in internal resistance (24 Ω) compared with the cells using the composite electrodes. This result also confirms here that the seamless structure in electrode contributes to the excellent durability against high voltage charging. Since the durability of the cell using gSEAMLESS composite electrode was much lower than that of SEAMLESS, the excellent durability of SEAMLESS is not derived from the porosity and carbon surface chemistry of the carbon material. These data suggest the following: in the composite electrode, electrochemical decomposition deposition (EDD) or the electrochemical destruction of the binder during the high voltage charge damages the electric contacts between particles of activated carbon and carbon black. This electric-network breakdown inside the electrode causes the marked increase in internal resistance. In contrast, the seamless activated carbon electrode is free from the electric-network breakdown. **Fig. S2** supports that the seamless structure for both SEAMLESS and AN-SEAMLESS was maintained even after the durability test. Therefore, the N-doping to the seamless activated carbon electrode is expected to improve the electrochemically durability furthermore in addition to the advantage of the seamless structure. In fact, the cell using AN-SEAMLESS shows higher retention (83%) and smaller change in internal resistance (11 Ω) than those of the cell using pristine SEAMLESS.

Then, to discuss the detail of the N-doping effect on the durability, the authors focus on the slope of the charge–discharge curve in **Fig. 4**. The capacitance retention in **Table II** is influenced by decrease in effective electrode surface area available to ion-adsorption/desorption and increase in electrode internal resistance, so it is necessary to separate them. The capacitance calculated from only curve slope (0–2 V) is directly related to the effective electrode surface area. These slope capacitances of pristine SEAMLESS and AN-SEAMLESS before the durability test are 31.5 F g^{-1} and 32.3 F g^{-1}, respectively. Those after the durability are 27.0 F g^{-1} and 29.2 F g^{-1}, thus the retention of the slope capacitance after the durability test for pristine SEAMLESS or AN-SEAMLESS are 86% or 90%, respectively. This suggests that the N-doping effect suppress the decrease of the effective surface area at high voltage charge. To evaluate the actual change in porous texture, the authors conducted N_2 adsorption/desorption measurements for the durability-tested electrodes. In the pore size distribution shown in **Fig. S4** calculated from **Fig. 2** and **Fig. S3**, the durability test did not shift the pore-width peak position, but decreased the pore volume. Therefore, the electrochemical decomposition deposits (EDD) would block the entrance of the pores to form "dead pore" illustrated in **Fig. 5a**. **Table III** shows the retention of the BET specific surface area and micropore volume calculated from **Fig. 2** and **Fig. S3**. These parameter retentions were higher in AN-SEAMLESS compared with pristine SEAMLESS. This result supports the retention of the slope capacitance and confirms that the N-doping suppress the pore blockage caused by the EDD during high voltage charging as shown in **Fig. 5a**.

Comparing the capacitance retention in **Table II** and the slope capacitance retention (effective surface area retention), only the suppression of micropore blockage proposed above cannot explain sufficiently the capacitance-retention improvement by the N-doping. The decrease in the internal resistance should be also connected to the improvement as shown in **Table II**. Then, the authors analyzed the change of the internal resistance by electrochemical impedance spectroscopy. **Fig. 6** shows the Nyquist plot (0 V, 40 °C, 1.0×10^{-2}–2.0×10^{3} Hz) before and after the durability test. For the cells using the seamless activated carbon electrodes, the Nyquist plot before the durability test consisted of a linear region of 45 ° on the high frequency side and a vertically rising line on the low frequency side. This is typical for EDLC and consistent with the transmission line (TML) model.[34,35]

However, a semicircle appeared after the durability test even in the cell using the seamless activated carbon electrodes. Generally, a semicircle on the high frequency side comes from the contact resistance (R_c) between particles such as activated carbon and conductive additive, or between active materials and current collector.[28] Since the seamless activated carbon electrodes intrinsically have no contact points inside the electrode, the arc should be assigned to the contact resistance on the interface between the collector and electrode. Here, the semicircle of the cell using AN-SEAMLESS is smaller than that of the cell using pristine SEAMLESS. This indicates that the N-doping suppresses the low-conductive EDD contributing to the contact resistance as shown in **Fig.5b**. The above discussion based on the Nyquist plot is consistent with the internal resistance calculated from the ohmic drop in Table II.

Fig. 7 shows the rate performance before and after the floating-durability test (3.5 V, 100 h, 70 °C). The initial volumetric capacitance in the case of the seamless activated carbon electrode was enough higher than that of YP50F-composite electrode. Also from the viewpoint of durability, the cell using pristine SEAMLESS showed very high capacitance retention compared with the cell using YP50F-composite electrode. Furthermore, AN-SEAMLESS achieved the excellent retention compared with pristine SEAMLESS. The effect of the N-doping was not lost even at high current density. That is, we succeeded in development of the electrode with both comparable volumetric capacitance and extremely high durability against high-voltage charge.

Conclusions [Required]

The authors prepared the N-doped seamless activated carbon electrode and investigated the capacitance performance in organic electrolyte. The conclusions were as follows:

i) The N-doping via organic chemical reaction is effective for further improving the durability of the EDLC using seamless activated carbon against high-voltage charge. This is because the N-doping suppresses the micropore blockage and internal-resistance increase caused by electrochemical decomposition during high-voltage charge.

ii) The EDLC using the N-doped seamless activated carbon shows comparable volumetric capacitance and higher rate-performance after the durability test (3.5 V, 70 °C, 100 h) compared with that using typical composite activated carbon electrode.

The authors believe that the strategy to combine monolithic electrode and N-doping will open new window for development of more durable and high-performance EDLC.

Acknowledgments [Optional]

This work is partially supported by JSPS KAKENHI Grant. No. 17H03123.

References [Required]

1. P. Simon and Y. Gogotsi, *Nat. Mater.*, **7** (11), 845–854 (2008).
2. W. Yang et al., *Curr. Opin. Colloid Interface Sci.*, **20**, 416–428 (2015).
3. S. Shiraishi, *Bol. Grupo Esp. Carbón*, **28**, 18–24 (2013).
4. S. Shiraishi, *Key Eng. Mater.*, **497**, 80–86 (2012).
5. Q. Meng, K. Cai, Y. Chen, and L. Chen, *Nano Energy*, **36**, 268–285 (2017).
6. A. Borenstein et al., *J. Mater. Chem. A*, **5** (25), 12653–12672 (2017).
7. S. Muroi et al., *Electrochemistry*, **83** (8), 609–618 (2015) (in Japanese).
8. S. Ishimoto, Y. Asakawa, M. Shinya, and K. Naoi, *J. Electrochem. Soc.*, **156** (7), A563–A571 (2009).
9. R. Tang et al., *J. Mater. Chem. A*, **7** (13), 7480–7488 (2019).
10. C. Zhong et al., *Chem. Soc. Rev.*, **44** (21), 7484–7539 (2015).
11. J. Krummacher, C. Schütter, L. H. Hess, and A. Balducci, *Curr. Opin. Electrochem.*, **9**, 64–69 (2018).
12. H.-H. Shen and C.-C. Hu, *J. Electroanal. Chem.*, **779**, 161–168 (2016).
13. T. Sato, G. Masuda, and K. Takagi, *Electrochimica Acta*, **49** (21), 3603–3611 (2004).
14. Y. Watanabe and S. Shiraishi, *Tanso*, **2019** (288), 128–134 (2019).
15. K. Chiba et al., *J. Electrochem. Soc.*, **158** (8), A872–A882 (2011).
16. A. Izadi-Najafabadi et al., *Adv. Mater.*, **22** (35), E235-241 (2010).
17. Y. Dong, Z.-S. Wu, W. Ren, H.-M. Cheng, and X. Bao, *Sci. Bull.*, **62** (10), 724–740 (2017).
18. H. Nishihara et al., *Adv. Funct. Mater.*, **26** (35), 6418–6427 (2016).
19. V. Ruiz et al., *Carbon*, **47** (1), 195–200 (2009).
20. A. Garcia-Gomez, P. Miles, T. A. Centeno, and J. M. Rojo, *Electrochem. Solid-State Lett.*, **13** (8), A112–A114 (2010).
21. Tsukada, Hidehiko, K. Onda, H. Miyaji, S. Shiraishi, and Y. Endo, WO2013140937A1 (2013).
22. H. Tsukada, K. Onda, H. Miyaji, S. Shiraishi, and Y. Endo, WO2015041051A1 (2015).
23. Y.-W. Chi, C.-C. Hu, H.-H. Shen, and K.-P. Huang, *Nano Lett.*, **16** (9), 5719–5727 (2016).

24. D. Cazorla-Amorós et al., *Carbon*, **48** (5), 1451–1456 (2010).
25. D. Salinas-Torres, S. Shiraishi, E. Morallón, and D. Cazorla-Amorós, *Carbon*, **82**, 205–213 (2015).
26. C.-H. Yang et al., *ACS Sustain. Chem. Eng.*, **6** (1), 1208–1214 (2018).
27. M. J. Mostazo-López, R. Ruiz-Rosas, E. Morallón, and D. Cazorla-Amorós, *Int. J. Hydrog. Energy*, **41** (43), 19691–19701 (2016).
28. W. Shen and W. Fan, *J. Mater. Chem. A*, **1** (4), 999–1013 (2012).
29. A. Chen et al., *ChemElectroChem*, **6** (2), 535–542 (2019).
30. A. Oya, S. Shiraishi, T. Tonouchi, Y. Ando, and T. Kyotani, JP 2008141116 A (2008).
31. S. Shiraishi, S. Kawaguchi, I. Shimabukuro, and Y. Hatakeyama, *Tanso*, **2019** (289), 139–147 (2019) (in Japanese).
32. S. Shiraishi et al., JP 2018219224 (2018).
33. S. Kundu et al., *Phys. Chem. Chem. Phys.*, **12** (17), 4351–4359 (2010).
34. Ishikawa M., *Electrochemistry*, **84**(12), 985–990 (2016) (in Japanese).
35. S. Dsoke, X. Tian, C. Täubert, S. Schlüter, and M. Wohlfahrt-Mehrens, *J. Power Sources*, **238**, 422–429 (2013).

Tables

Table I. The pore structure and chemical composition of SEAMLESS, AN-SEAMLESS, YP50F.

Sample	S_{BET}[a] [$m^2\ g^{-1}$]	V_{micro}[b] [$cm^3\ g^{-1}$]	w_{micro}[c] [nm]	O_{diff}/C_{comb}[d] [at%]	N/C_{comb}[e] [at%]	O/C_{xps}[f] [at%]	N/C_{xps}[g] [at%]
SEAMLESS	1720	0.68	0.96	13	0.28	8.9	0
AN-SEAMLESS	1670	0.66	0.93	5.2	1.0	5.1	2.7
YP50F	1620	0.68	1.1	2.5	0.1	–	–

[a] S_{BET}: BET specific surface area

[b] V_{micro}: Volume of micropore

[c] w_{micro}: mean micropore width

[d] $O_{diff}/C_{combust.}$: Oxygen content per carbon content by combustion analysis, where oxygen content was estimated by subtracting carbon and nitrogen content from the whole.

[e] $N/C_{combust.}$: Nitrogen content per carbon content.

[f] O/C_{xps}: Oxygen content per carbon content estimated by XPS analysis.

[g] O/N_{xps}: Nitrogen content per carbon content estimated by XPS analysis.

Table II. Capacitance, leakage current, and internal resistance associated with durability test (3.5 V, 100 h, 70 °C).

Sample	C_i[a] [$F\ g^{-1}$]	C_f/C_i[b] [%]	ILC[c] [$mA\ h\ g^{-1}$]	R_i[d] [Ω]	ΔR[e] [Ω]	d[f] [$g\ cm^{-3}$]
SEAMLESS	32	76	460	3	24	0.56
AN-SEAMLESS	32	83	440	4	11	0.56
YP50F (composite)	26	1	320	3	321	0.64
gSEAMLESS (composite)	32	17	420	4	86	0.51

[b] C_f/C_i: Capacitance retention before/after durability test.

[c] ILC: Integrated leakage current during the durability test.

[d] R_i: Initial resistance.

[e] ΔR: increase of internal resistance.

[f] d: Bulk density.

Table III. The retention of porosity properties before and after durability test (3.5 V, 100 h, 70 °C).

Sample	S_{BET}[a] [%]	V_{micro}[b] [%]
Tested SEAMLESS (+)	65	62
Tested AN-SEAMLESS (+)	68	67
Tested SEAMLESS (−)	74	72
Tested AN-SEAMLESS (−)	75	74

[a]S_{BET}: Retention of BET specific surface area [m^2 g^{-1}] before and after durability test **(3.5 V, 100 h, 70 °C).**

[b]V_{micro}: Retention of micropore volume [cm^3 g^{-1}] before and after durability test **(3.5 V, 100 h, 70 °C).**

Figure Captions

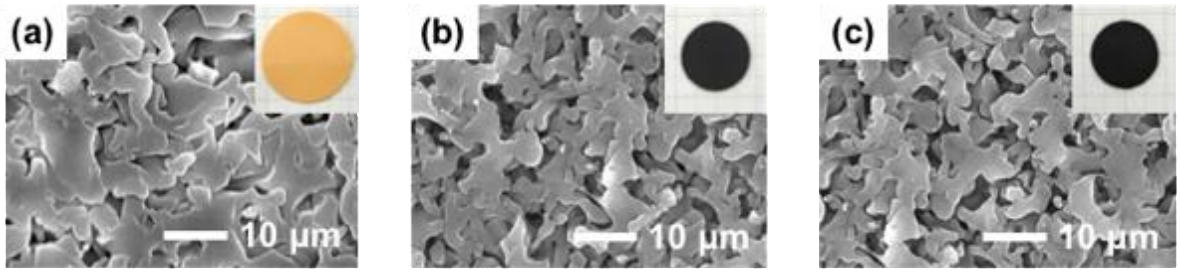

Fig.1 SEM image and appearance (inset) of (a) macroporous phenolic resin disk, (b) seamless activated carbon electrode (SEAMLESS), or (c) nitrogen-doped seamless activated carbon electrode (AN- SEAMLESS).

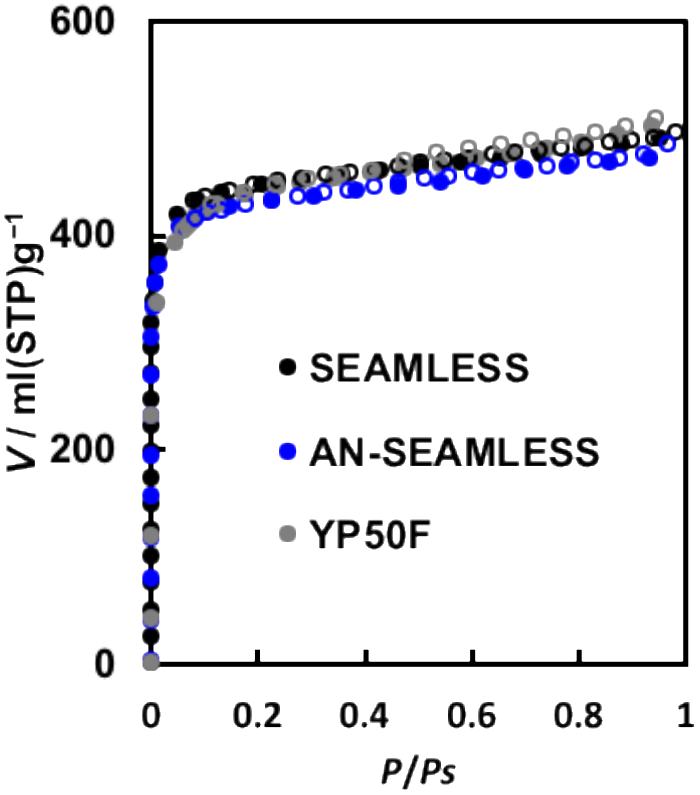

Fig.2 N_2 adsorption/desorption isotherms at 77 K of seamless activated carbon (SEAMLESS) , N-doped seamless activated carbon (AN-SEAMLESS), and YP50F.

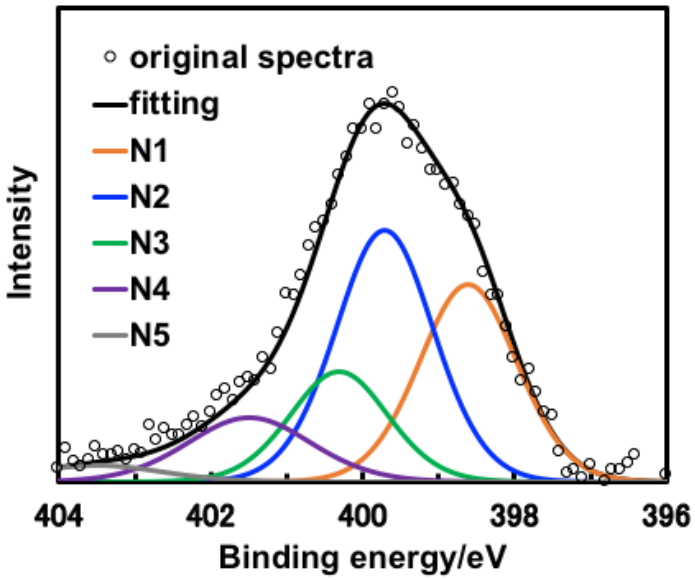

Fig. 3 N1s XPS spectra of AN-SEAMLESS.

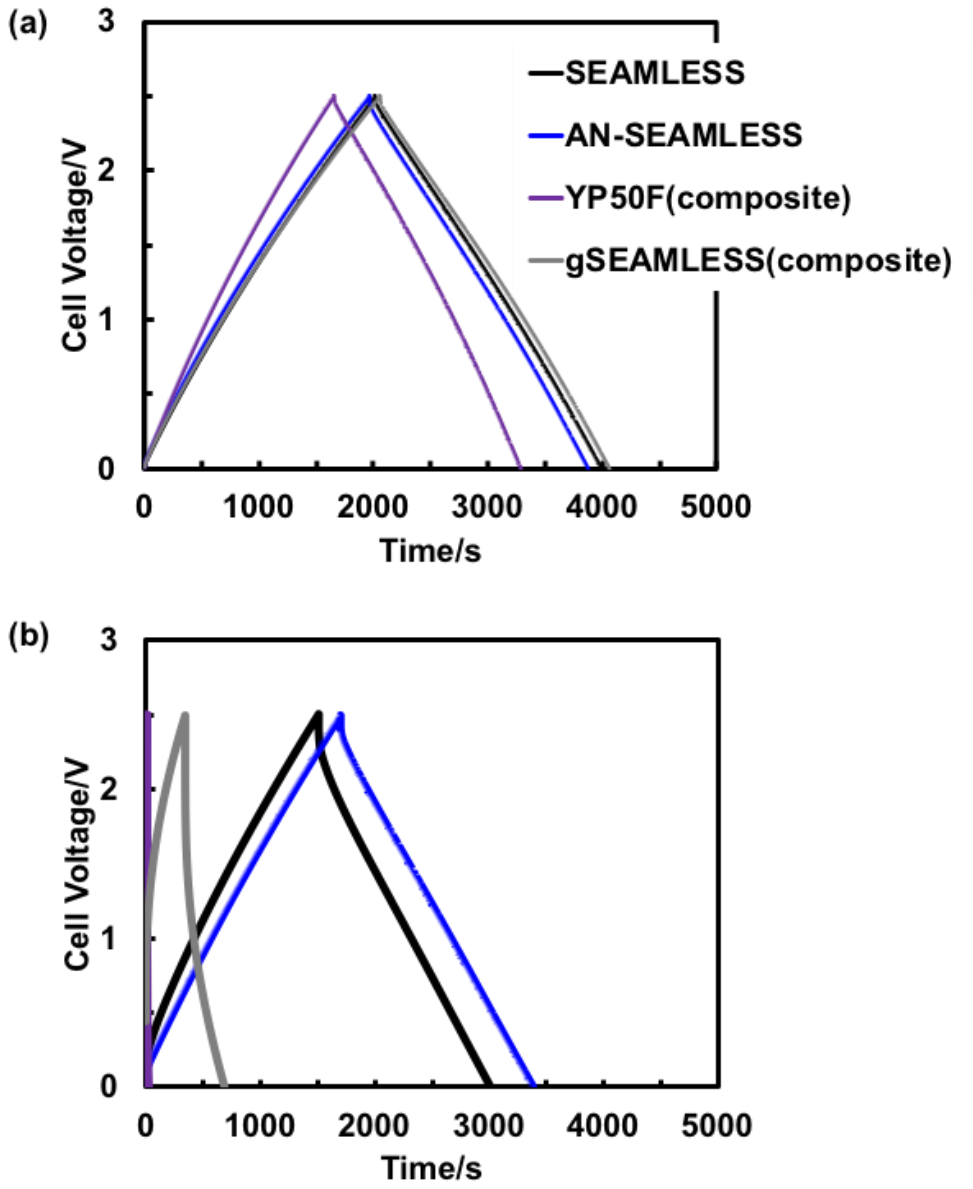

Fig. 4 Charge–discharge Curve (a) before and (b) after floating durability test (3.5 V, 100 h, 70 °C). 1 M $TEMABF_4$/PC, Two-electrode cell, 80 mA g^{-1} 40 ˚C, 0–2.5 V.

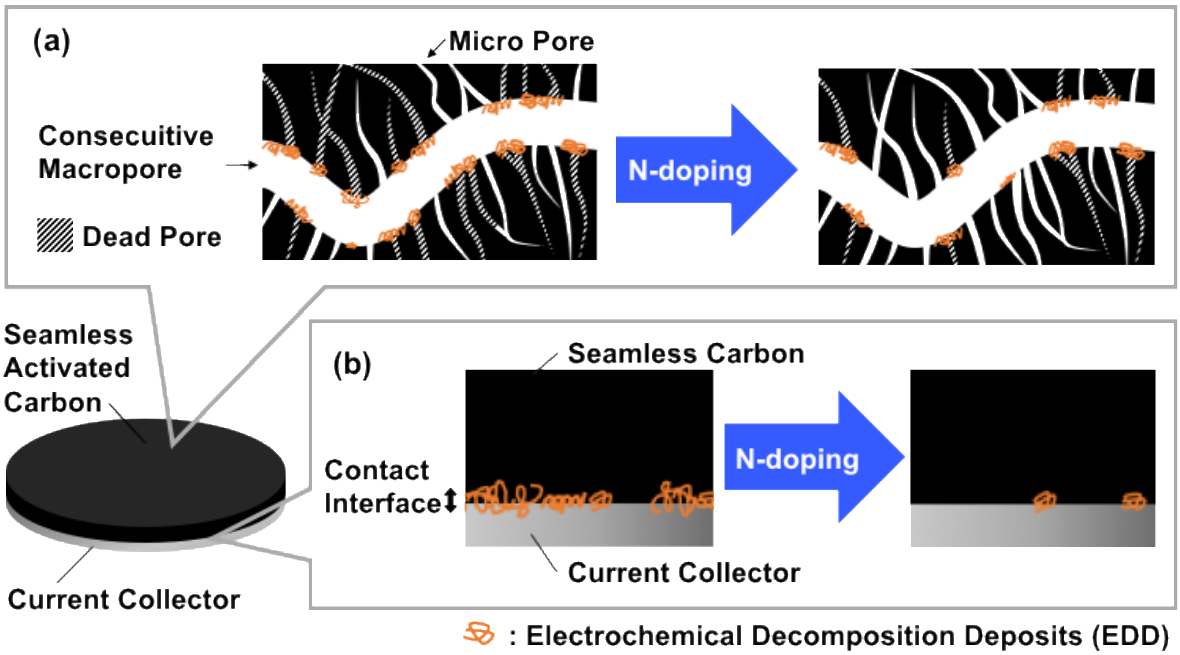

Fig. 5 Model of (a) pore blocking and (b) contact resistance caused by electrochemical decomposition deposits (EDD) on tested electrodes.

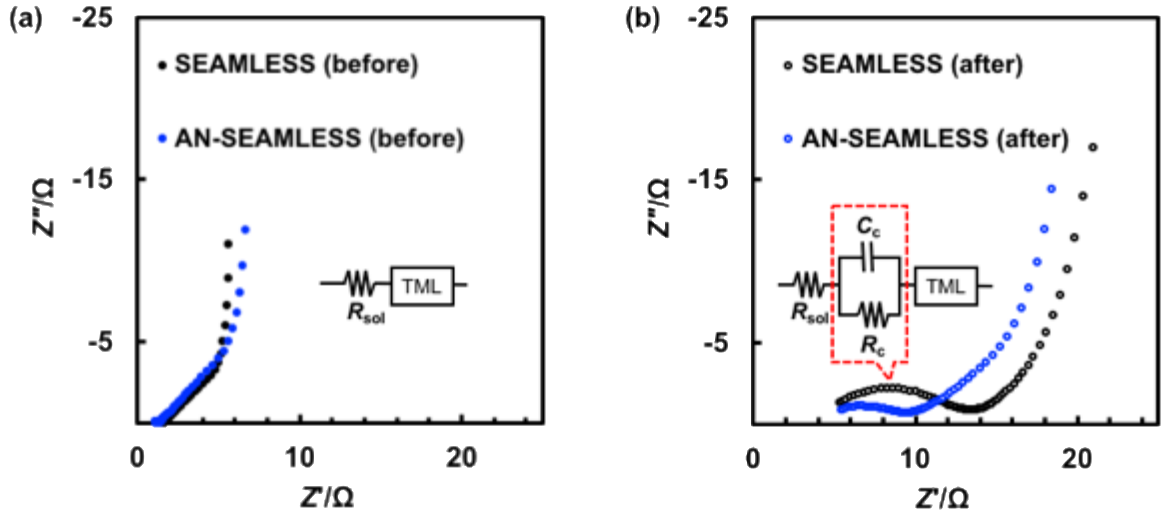

Fig. 6 Nyquist plot (a) before and (b) after floating durability test (3.5 V, 100 h, 70 °C). 1 M $TEMABF_4$/PC, Two-electrode cell, 40 ˚C, 0 V, 1.0×10─2–2×103 Hz.

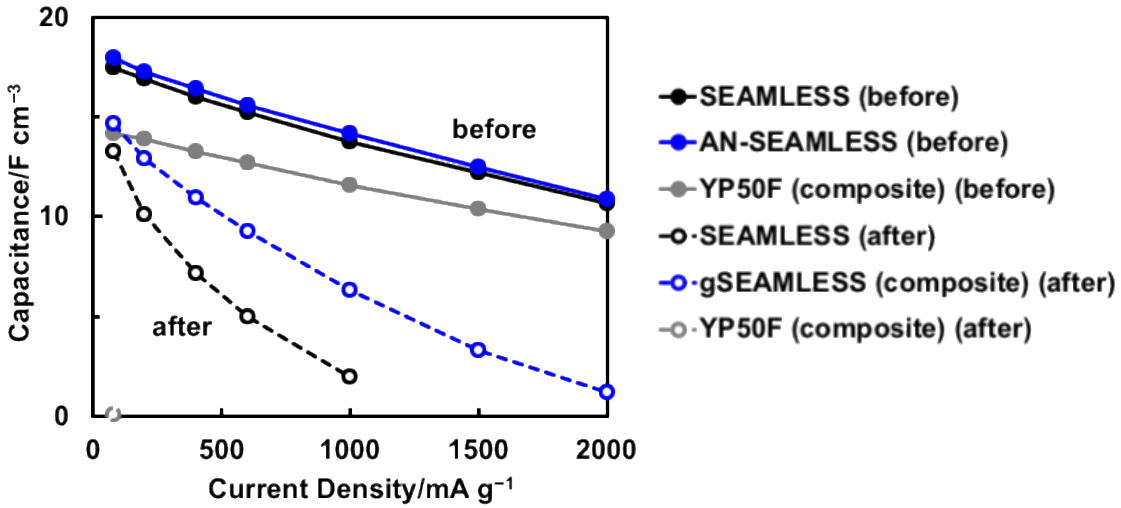

Fig. 7 Rate performance before and after floating durability test (3.5 V, 100 h, 70 °C). 1 M $TEMABF_4$/PC, Two-electrode cell, 80 mA g^{-1} 40 ˚C, 0–2.5 V.

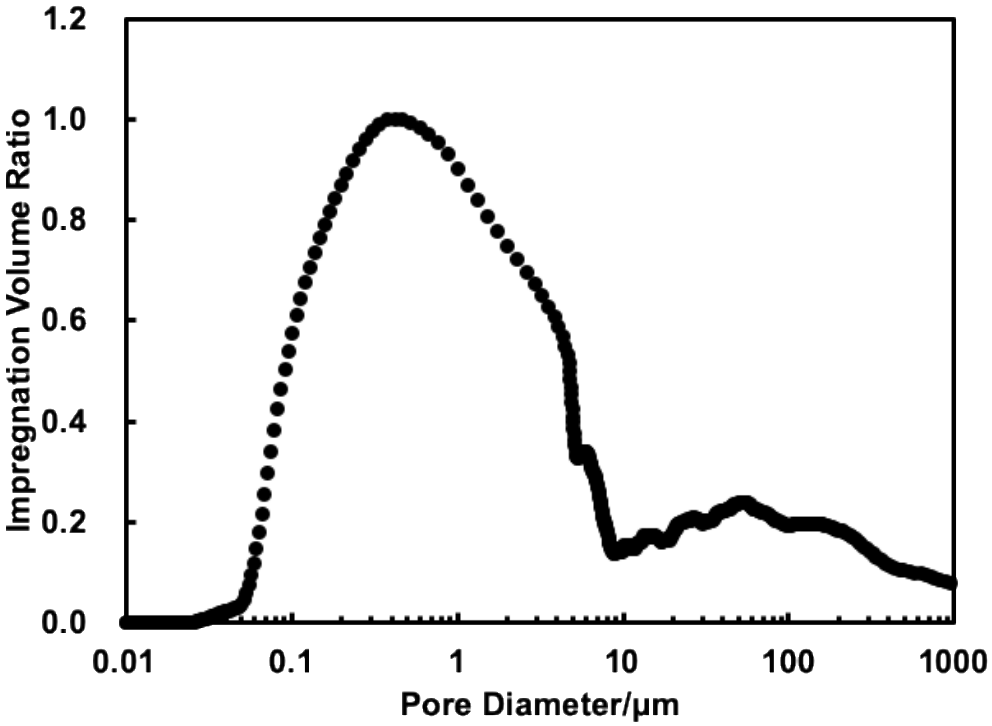

Fig. S1 Macropore distribution of macroporous phenolic resin (densified MICROLITE, produced by AION Co. Ltd., Japan) determined by mercury porosimetry.

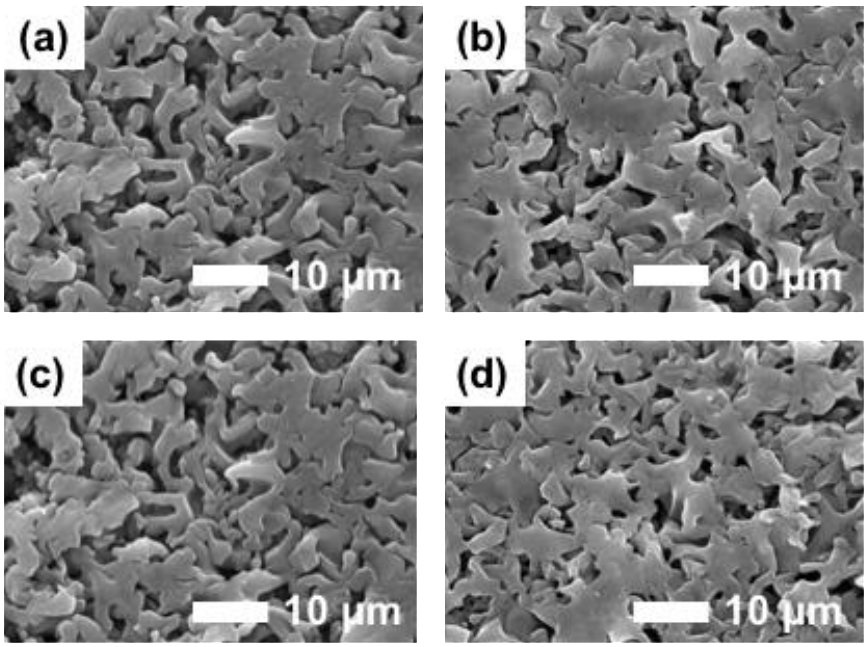

Fig. S2 SEM image of (a) Tested SEAMLESS (+), (b) Tested SEAMLESS (−), (c) Tested AN-SEAMLESS(+), (d) Tested AN-SEAMLESS(−).

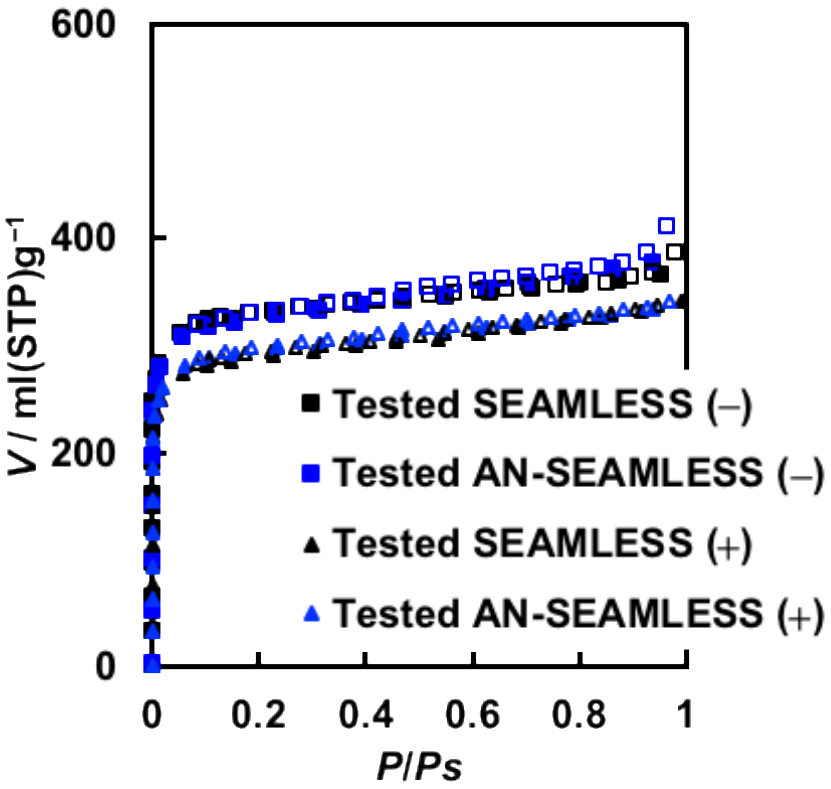

Fig. S3 N_2 adsorption/desorption isotherms at 77 K of activated carbons SEAMLESS and AN-SEAMLESS after durability test (3.5 V, 100 h, 70 °C).

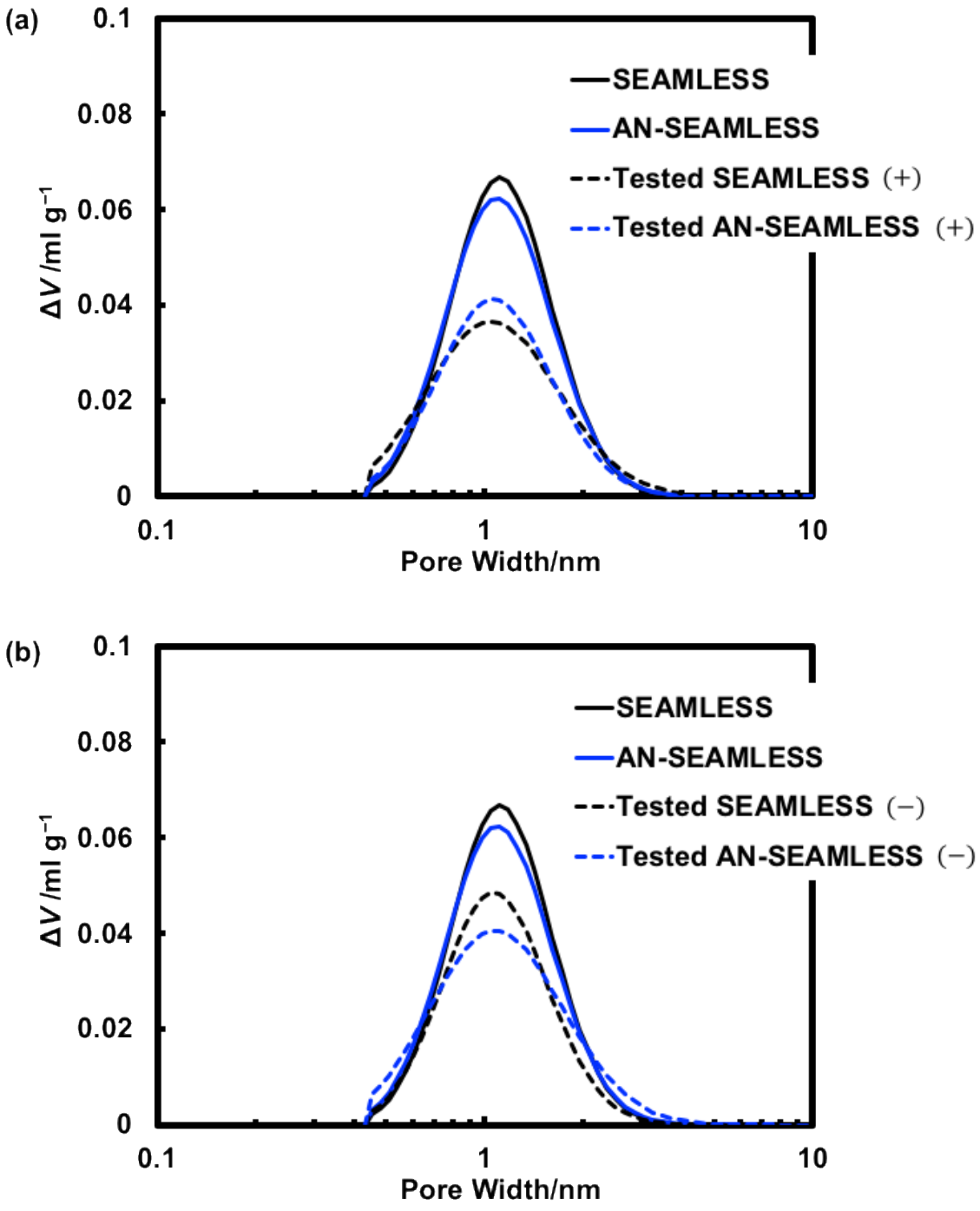

Fig. S4 Pore size distribution calculated based on the non-local density functional theory (NLDFT) from N_2 adsorption/desorption isotherms at 77 K for SEAMLESS and AN-SEAMLESS after durability test (3.5 V, 100 h, 70 °C).